

RMT: Retentive Networks Meet Vision Transformers

Qihang Fan^{1,2,3}, Huaibo Huang^{1,2}, Mingrui Chen^{1,2,3}, Hongmin Liu⁴, Ran He^{1,2,3*}

¹Center for Research on Intelligent Perception and Computing, CASIA, Beijing, China

²National Laboratory of Pattern Recognition, CASIA, Beijing, China

³School of Artificial Intelligence, University of Chinese Academy of Sciences, Beijing, China

⁴University of Science and Technology Beijing, Beijing, China

fanqihang.159@gmail.com, huaibo.huang@cripac.ia.ac.cn,
charmier@hust.edu.cn, hmliu_82@163.com, rhe@nlpr.ia.ac.cn

Abstract

Transformer first appears in the field of natural language processing and is later migrated to the computer vision domain, where it demonstrates excellent performance in vision tasks. However, recently, Retentive Network (RetNet) has emerged as an architecture with the potential to replace Transformer, attracting widespread attention in the NLP community. Therefore, we raise the question of whether transferring RetNet's idea to vision can also bring outstanding performance to vision tasks. To address this, we combine RetNet and Transformer to propose RMT. Inspired by RetNet, RMT introduces explicit decay into the vision backbone, bringing prior knowledge related to spatial distances to the vision model. This distance-related spatial prior allows for explicit control of the range of tokens that each token can attend to. Additionally, to reduce the computational cost of global modeling, we decompose this modeling process along the two coordinate axes of the image. Abundant experiments have demonstrated that our RMT exhibits exceptional performance across various computer vision tasks. For example, RMT achieves 84.1% Top1-acc on ImageNet-1k using merely 4.5G FLOPs. To the best of our knowledge, among all models, RMT achieves the highest Top1-acc when models are of similar size and trained with the same strategy. Moreover, RMT significantly outperforms existing vision backbones in downstream tasks such as object detection, instance segmentation, and semantic segmentation. Our work is still in progress.

1. Introduction

Since the Transformer was proposed in the field of NLP[52], it has achieved outstanding performance in many downstream tasks. Despite the modality gap between com-

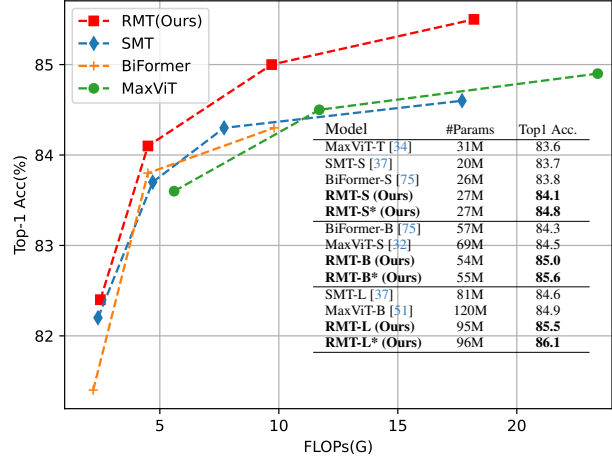


Figure 1. FLOPs vs. Top-1 accuracy on ImageNet-1K with 224×224 resolution. “*” indicates the model trained with token labeling [30].

puter vision and natural language processing, researchers have successfully migrated this architecture to vision tasks, bringing us once again a huge surprise like in previous NLP tasks[3, 12, 13, 28, 34].

Recently, several powerful architectures [43, 48] have emerged in the NLP community, yet no work has attempted to transfer these NLP architectures to visual tasks. Compared to Transformer, Retentive Network (RetNet) [48] has demonstrated stronger performance on a range of NLP tasks. Therefore, we hope to be able to transfer this robust NLP architecture, RetNet, to the domain of vision.

The fundamental operator in RetNet is retention. A significant difference between retention and the basic Self-Attention operator in Transformer is the introduction of decay coefficients, which explicitly control the attention weights of each token with respect to its neighboring tokens, ensuring that the attention weights decay as the distance between tokens increases. This decay effectively introduces prior knowledge about one-dimensional distance

*Ran He is the corresponding author.

into the model, resulting in improved performance.

Based on the findings in RetNet, we attempt to further improve retention into a 2D form and introduce it to visual tasks. Specifically, the original version of retention undergoes unidirectional decay, which suits the causal properties of NLP. However, for images without causal properties, this unidirectional decay is not suitable. Therefore, we first expand retention from unidirectional to bidirectional. Additionally, the original version of retention, designed for one-dimensional sequential information, is not appropriate for use in two-dimensional space. Hence, considering the spatial characteristics of two dimensions, we design a decay matrix based on 2D distance. Finally, to address the high computational load caused by a large number of tokens during the early stage of the vision backbone, we decompose the 2D computation process separately along the two axes of the image. We name this mechanism adapted to images as the **Retentive Self-Attention (ReSA)** mechanism. Based on the ReSA mechanism, we construct the RMT family.

We demonstrate the effectiveness of the proposed method through extensive experiments. As shown in Fig. 1, our RMT significantly outperforms the state-of-the-art (SOTA) models on image classification tasks. Additionally, our model exhibits more prominent advantages compared to other models in tasks such as object detection and instance segmentation. Our contributions can be summarized as follows:

- We extend the core mechanism of the Retentive Network, retention, to the two-dimensional scenario, introducing spatial prior knowledge related to distances into vision models. The new mechanism is called Retentive Self-Attention (ReSA).
- We decompose ReSA along two image axes, reducing computational complexity. This decomposition method effectively minimizes the computational burden while having minimal impact on the model’s performance.
- Extensive experiments demonstrate the excellent performance of RMT. Particularly in downstream tasks such as object detection and instance segmentation, RMT exhibits significant advantages.

2. Related Work

Transformer. Transformer architecture was firstly proposed in [52] to address the training limitation of recurrent model and then achieve massive success in many NLP tasks. By splitting the image into small, non-overlapped patches sequence, Vision Transformer (ViTs) [12] also have attracted great attention and become widely used on vision tasks [5, 16, 20, 42, 58, 66]. Unlike in the past, where RNNs and CNNs have respectively dominated the NLP and CV fields, the transformer architecture has shined through in various modalities and fields [29, 40, 44, 60].

Prior Knowledge in Transformer. Numerous attempts have been made to incorporate prior knowledge into the Transformer model to enhance its performance. The original Transformers [12, 52] use trigonometric position encoding to provide positional information for each token. [38] proposes the use of relative positional encoding as a replacement for the original absolute positional encoding. [6] points out that zero padding in convolutional layers could also provide positional awareness for the Transformer, and this method of position encoding is highly efficient. In many studies, ConvFFN [14, 15, 18, 54] has been employed to further enrich the positional information in the Transformer. Furthermore, in the recent Retentive Network [48], explicit attenuation has been introduced to provide the model with prior knowledge based on distance changes.

Retentive Network. Retentive Network [48] proposes the retention mechanism for sequence modeling. Compared to traditional Transformer based models [11, 12, 28, 38, 52], retention proposed in RetNet uses the explicit decay to model the prior of 1D distance. It includes three computation paradigms, i.e., parallel, recurrent, and chunkwise recurrent. In retention, it uses a decay matrix multiplied by a weight matrix to control the proportion of each token seeing its surrounding tokens based on distance priors. We attempt to extend this idea to 2D space.

3. Methodology

3.1. Preliminary

Retentive Network. Retentive Network (RetNet) is a powerful architecture for language models. This work proposes the retention mechanism for sequence modeling. Retention brings the explicit decay to the language model, which Transformers do not have. Retention firstly considers a sequence modeling problem in a recurrent manner. It can be written as Eq. 1:

$$o_n = \sum_{m=1}^n \gamma^{n-m} (Q_n e^{in\theta}) (K_m e^{im\theta})^\dagger v_m \quad (1)$$

During training, for a parallel training process, Eq. 1 is written as Eq. 2:

$$\begin{aligned} Q &= (XW_Q) \odot \Theta, \quad K = (XW_K) \odot \overline{\Theta}, \quad V = XW_V \\ \Theta_n &= e^{in\theta}, \quad D_{nm} = \begin{cases} \gamma^{n-m}, & n \geq m \\ 0, & n < m \end{cases} \\ \text{Retention}(X) &= (QK^\top \odot D)V \end{aligned} \quad (2)$$

where $\overline{\Theta}$ is the complex conjugate of Θ , and $D \in \mathbb{R}^{|x| \times |x|}$ contains both causal masking and exponential decay, which

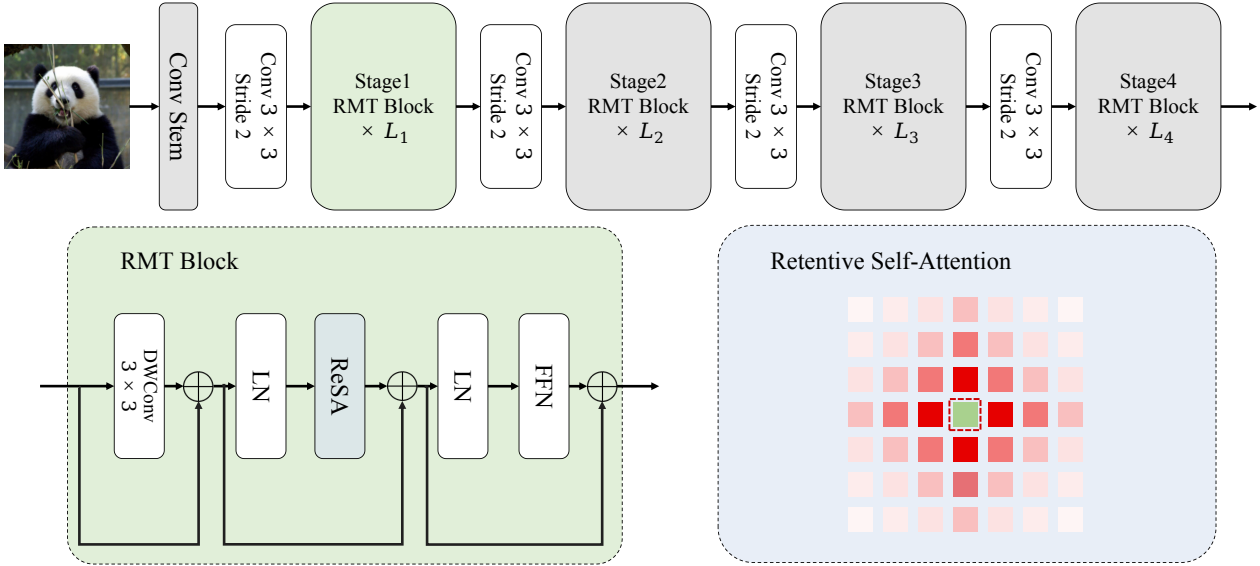


Figure 2. Overall architecture of RMT.

symbolize the relative distance in one-dimensional sequence, which brings the prior knowledge. Based on the 1D explicit decay in the retention, we try to develop it to 2D and bring the spatial prior knowledge to the vision model.

3.2. Retentive Self-Attention

Unidirectional to Bidirectional. Due to the causal nature of language tasks, the retention in RetNet is unidirectional, meaning that each token can only attend to the tokens preceding it and not those following it. This is not suitable for tasks without causal properties, such as image recognition tasks. Therefore, we first extend the retention to two dimensions, where for each token, its output becomes Eq. 3:

$$o_n = \sum_{m=1}^N \gamma^{|n-m|} (Q_n e^{in\theta}) (K_m e^{im\theta})^\dagger v_m \quad (3)$$

where N is the number of tokens. The equation can be rearranged into a parallel form, expressed as Eq. 4:

$$\begin{aligned} \text{BiRetention}(X) &= (QK^\top \odot D^{Bi})V \\ D_{nm}^{Bi} &= \gamma^{|n-m|} \end{aligned} \quad (4)$$

where BiRetention denotes the retention with bidirectional modeling ability.

1D to 2D. Although retention now has the ability for bidirectional modeling, this modeling capability remains limited to a one-dimensional level and is still not applicable to two-dimensional images. Therefore, we further extend the one-dimensional retention to two dimensions.

For images, each token has a unique two-dimensional coordinate within the plane. For the n th token, we use

(x_n, y_n) to represent its two-dimensional coordinate. Based on the 2D coordinates of each token, we modify each element in the matrix D to be the Manhattan distance between the corresponding token pairs at their respective positions, completing the transformation from a 1D to a 2D decay coefficient. The matrix D transfers to Eq. 5:

$$D_{nm}^{2d} = \gamma^{|x_n - x_m| + |y_n - y_m|} \quad (5)$$

In the retention [48], the Softmax is abandoned and replaced with a gating function to increase the nonlinearity of the operator. However, according to our experiments, this approach does not yield better results for vision models. Instead, it introduces additional parameters and computational complexity. Therefore, we still use Softmax to introduce nonlinearity to our model. Based on the steps mentioned above, our Retentive Self-Attention can be expressed as Eq. 6:

$$\begin{aligned} \text{ReSA}(X) &= (\text{Softmax}(QK^\top) \odot D^{2d})V \\ D_{nm}^{2d} &= \gamma^{|x_n - x_m| + |y_n - y_m|} \end{aligned} \quad (6)$$

Decomposed ReSA in Early Stage. The current ReSA is not entirely applicable to image recognition tasks. This is because, in the early stages of the vision backbone, there are a large number of tokens, resulting in excessive computational costs for Attention. This is also the problem that most variants of Vision Transformers strive to solve [46, 57, 58, 61, 66, 72].

Our ReSA also encounters this problem. Therefore, we decompose ReSA into two axes of the image, as described

Cost	Model	Parmas (M)	FLOPs (G)	Top1-acc (%)	Cost	Model	Parmas (M)	FLOPs (G)	Top1-acc (%)
tiny model ~ 2.5G	PTV2-b1 [54]	13	2.1	78.7	base model ~ 9.0G	ConvNeXt-S [39]	50	8.7	83.1
	QuadTree-B-b1 [49]	14	2.3	80.0		CrossFormer-B [55]	52	9.2	83.4
	RegionViT-T [3]	14	2.4	80.4		InceptionNeXt-S [68]	49	8.4	83.5
	MPViT-XS [32]	11	2.9	80.9		NAT-S [21]	51	7.8	83.7
	tiny-MOAT-2 [62]	10	2.3	81.0		Quadtree-B-b4 [49]	64	11.5	84.0
	VAN-B1 [19]	14	2.5	81.1		Ortho-B [27]	50	8.6	84.0
	BiFormer-T [75]	13	2.2	81.4		ScaleViT-B [65]	81	8.6	84.1
	Conv2Former-N [25]	15	2.2	81.5		MOAT-1 [62]	42	9.1	84.2
	CrossFormer-T [55]	28	2.9	81.5		InternImage-S [56]	50	8.0	84.2
	NAT-M [21]	20	2.7	81.8		DaViT-S [10]	50	8.8	84.2
	QnA-T [1]	16	2.5	82.0		GC-ViT-S [22]	51	8.5	84.3
	GC-ViT-XT [22]	20	2.6	82.0		BiFormer-B [75]	57	9.8	84.3
	SMT-T [37]	12	2.4	82.2		MViTv2-B [34]	52	10.2	84.4
	RMT-T	14	2.5	82.4		CMT-B [18]	46	9.3	84.5
						iFormer-B [47]	48	9.4	84.6
						RMT-B	54	9.7	85.0
small model ~ 4.5G	DeiT-S [50]	22	4.6	79.9	large model ~ 18.0G	DeiT-B [50]	86	17.5	81.8
	Swin-T [38]	29	4.5	81.3		Swin-B [38]	88	15.4	83.3
	ConvNeXt-T [39]	29	4.5	82.1		LITv2 [42]	87	13.2	83.6
	Focal-T [63]	29	4.9	82.2		CrossFormer-L [55]	92	16.1	84.0
	InceptionNeXt-T [68]	28	4.2	82.3		Ortho-L [27]	88	15.4	84.2
	FocalNet-T [64]	29	4.5	82.3		CSwin-B [11]	78	15.0	84.2
	RegionViT-S [3]	31	5.3	82.6		MPViT-B [32]	75	16.4	84.3
	CSWin-T [11]	23	4.3	82.7		ScalableViT-L [65]	104	14.7	84.4
	MPViT-S [32]	23	4.7	83.0		SMT-L [37]	81	17.7	84.6
	ScalableViT-S [65]	32	4.2	83.1		DaViT-B [10]	88	15.5	84.6
	SG-Former-S [17]	23	4.8	83.2		MOAT-2 [62]	73	17.2	84.7
	MOAT-0 [62]	28	5.7	83.3		SG-Former-B [17]	78	15.6	84.7
	Ortho-S [27]	24	4.5	83.4		iFormer-L [47]	87	14.0	84.8
	InternImage-T [56]	30	5.0	83.5		CMT-L [18]	75	19.5	84.8
	GC-ViT-T [22]	28	4.7	83.5		InterImage-B [56]	97	16.0	84.9
	CMT-S [18]	25	4.0	83.5		MaxViT-B [51]	120	23.4	84.9
	MaxViT-T [51]	31	5.6	83.6		GC-ViT-B [22]	90	14.8	85.0
	SMT-S [37]	20	4.8	83.7		RMT-L	95	18.2	85.5
	BiFormer-S [75]	26	4.5	83.8					
	RMT-S	27	4.5	84.1					

Table 1. Comparison with the state-of-the-art on ImageNet-1K classification.

in the specific process shown in Eq. 7:

$$\begin{aligned}
 Q_H, K_H &= (Q, K)^{B, L, C \rightarrow B, W, H, C} \\
 Q_W, K_W &= (Q, K)^{B, L, C \rightarrow B, H, W, C} \\
 Attn_H &= \text{Softmax}(Q_H K_H^\top) \odot D^H \\
 Attn_W &= \text{Softmax}(Q_W K_W^\top) \odot D^W \\
 D_{nm}^H &= \gamma^{|y_n - y_m|}, D_{nm}^W = \gamma^{|x_n - x_m|} \\
 \text{ReSA}_{\text{dec}}(X) &= Attn_H(Attn_W V)
 \end{aligned} \tag{7}$$

Based on this decomposition of ReSA, the shape of the receptive field of each token is shown in Fig. 3, which is identical to the shape of the complete ReSA’s receptive field.

In order to further enhance the local expression capability of ReSA, we also introduce a local enhancement module using DWConv:

$$X_{out} = \text{ReSA}(X) + \text{LCE}(X); \tag{8}$$

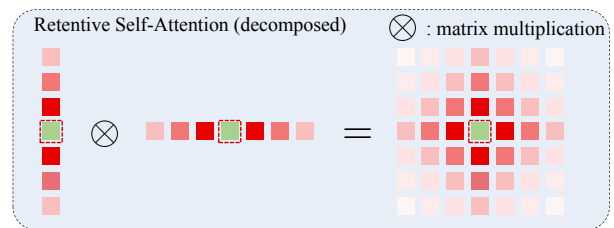


Figure 3. Illustration of decomposed ReSA.

3.3. Overall Architecture

The architecture of our entire model is shown in Fig 2. Similar to traditional backbones, it is divided into four stages. The first three stages utilize the decomposed ReSA, while the last stage uses the original ReSA. Like many previous backbones [18, 33, 75], we incorporate CPE [6] into our model.

Cost	Model	Params (M)	FLOPs (G)	Top1-acc (%)
small model ~ 4.5G	LV-ViT-S* [30]	26	6.6	83.3
	UniFormer-S* [33]	24	4.2	83.4
	WaveViT-S* [66]	23	4.7	83.9
	Dual-ViT-S* [67]	25	5.4	84.1
	VOLO-D1* [69]	27	6.8	84.2
	BiFormer-S* [75]	26	4.5	84.3
	RMT-S*	27	4.5	84.8
base model ~ 9.0G	LV-ViT-M* [30]	56	16.0	84.1
	WaveViT-B* [66]	34	7.2	84.8
	UniFormer-B* [33]	50	8.3	85.1
	VOLO-D2* [69]	59	14.1	85.2
	Dual-ViT-B* [67]	43	9.3	85.2
	BiFormer-B*	58	9.8	85.4
	RMT-B*	55	9.7	85.6
large model ~ 18.0G	LV-ViT-L* [30]	150	59.0	85.3
	VOLO-D3*	86	20.6	85.4
	WaveViT-L* [66]	58	14.8	85.5
	UniFormer-L* [33]	100	12.6	85.6
	Dual-ViT-L* [67]	73	18.0	85.7
	RMT-L*	96	18.2	86.1

Table 2. Models trained with additional supervision. “*” indicates the model trained with token labeling [30].

4. Experiments

We conducted extensive experiments on multiple vision tasks, such as image classification on ImageNet-1K [9], object detection and instance segmentation on COCO 2017 [36], and semantic segmentation on ADE20K [74]. We also make ablation studies to validate the importance of each component in RMT.

4.1. Image Classification

Settings. We train our models on ImageNet-1K [9] from scratch. And we follow the same training strategy in DeiT [50] for a fair comparison. The maximum rates of increasing stochastic depth [26] are set to 0.1/0.15/0.4/0.5 for RMT-T/S/B/L [26], respectively. We use the AdamW optimizer with a cosine decay learning rate scheduler to train the models. We set the initial learning rate, weight decay, and batch size to 0.001, 0.05, and 1024, respectively. We adopt the strong data augmentation and regularization used in [38]. Our settings are RandAugment [8] (randm9-mstd0.5-inc1), Mixup [71] (prob=0.8), CutMix [70] (prob=1.0), Random Erasing [73] (prob=0.25). In addition to the conventional training methods, similar to LV-ViT [30] and VOLO [69], we further train a model that utilizes token labeling to provide supplementary supervision.

Results. We compare RMT against many state-of-the-art models in Tab. 1. Results in the table demonstrate that RMT

consistently outperforms previous models across all settings. Specifically, RMT-S achieves **84.1%** Top1-accuracy with only **4.5** GFLOPs. RMT-B also surpasses iFormer [47] by **0.4%** with similar FLOPs. Furthermore, our RMT-L model surpasses MaxViT-B [51] in top1-accuracy by **0.6%** while using fewer FLOPs. Our RMT-T has also outperformed many lightweight models. As for the model trained using token labeling, our RMT-S outperforms the current state-of-the-art BiFormer-S by 0.5

4.2. Object Detection and Instance Segmentation

Settings. We adopt MMDetection [4] to implement RetinaNet [35] Mask-RCNN [24] and Cascade Mask R-CNN [2]. We use the commonly used “1×” (12 training epochs) setting for the RetinaNet and Mask R-CNN. Besides, we use “3 × +MS” for Mask R-CNN and Cascade Mask R-CNN. Following [38], during training, images are resized to the shorter side of 800 pixels while the longer side is within 1333 pixels. We adopt the AdamW optimizer with a learning rate of 0.0001 and batch size of 16 to optimize the model. For “1×” schedule, the learning rate declines with the decay rate of 0.1 at the epoch 8 and 11. While for “3 × +MS” schedule, the learning rate declines with the decay rate of 0.1 at the epoch 27 and 33.

Results. Tab. 3, Tab. 4 and Tab. 5 show the results with different detection frameworks. The results demonstrate that our RMT performs best in all comparisons. For the RetinaNet framework, our RMT-T outperforms FAT-B2 by **+1.1** AP, while S/B/L also perform better than other methods. As for the Mask R-CNN with “1×” schedule, RMT-L outperforms the recent InternImage-B by **+1.8** box AP and **+1.9** mask AP. For “3 × +MS” schedule, RMT-S outperforms InternImage-T for **+1.6** box AP and **+1.2** mask AP. Besides, when it comes to the Cascade Mask R-CNN, our RMT still performs much better than other backbones. All above results tell that RMT outperforms its counterparts by evident margins.

4.3. Semantic Segmentation

Settings. We adopt the Semantic FPN [31] and UperNet [59] based on MMSegmentation [7], apply RMTs which are pretrained on ImageNet-1K as backbone. We use the same setting of PVT [53] to train the Semantic FPN, and we train the model for 80k iterations. All models are trained with the input resolution of 512×512 . When testing the model, we resize the shorter side of the image to 512 pixels. As for UperNet, we follow the default settings in Swin [38]. We take AdamW with a weight decay of 0.01 as the optimizer to train the models for 160K iterations. The learning rate is set to 6×10^{-5} with 1500 iterations warmup.

Backbone	Params FLOPs		Mask R-CNN 1×						Params FLOPs		RetinaNet 1×					
	(M)	(G)	AP^b	AP_{50}^b	AP_{75}^b	AP^m	AP_{50}^m	AP_{75}^m	(M)	(G)	AP^b	AP_{50}^b	AP_{75}^b	AP_S^b	AP_M^b	AP_L^b
PVT-T [53]	33	240	39.8	62.2	43.0	37.4	59.3	39.9	23	221	39.4	59.8	42.0	25.5	42.0	52.1
PVTv2-B1 [54]	33	243	41.8	54.3	45.9	38.8	61.2	41.6	23	225	41.2	61.9	43.9	25.4	44.5	54.3
MPViT-XS [32]	30	231	44.2	66.7	48.4	40.4	63.4	43.4	20	211	43.8	65.0	47.1	28.1	47.6	56.5
FAT-B2 [15]	33	215	45.2	67.9	49.0	41.3	64.6	44.0	23	196	44.0	65.2	47.2	27.5	47.7	58.8
RMT-T	33	218	47.1	68.8	51.7	42.6	65.8	45.9	23	199	45.1	66.2	48.1	28.8	48.9	61.1
Swin-T [38]	48	267	43.7	66.6	47.7	39.8	63.3	42.7	38	248	41.7	63.1	44.3	27.0	45.3	54.7
CMT-S [18]	45	249	44.6	66.8	48.9	40.7	63.9	43.4	44	231	44.3	65.5	47.5	27.1	48.3	59.1
CrossFormer-S [55]	50	301	45.4	68.0	49.7	41.4	64.8	44.6	41	272	44.4	65.8	47.4	28.2	48.4	59.4
ScalableViT-S [65]	46	256	45.8	67.6	50.0	41.7	64.7	44.8	36	238	45.2	66.5	48.4	29.2	49.1	60.3
MPViT-S [32]	43	268	46.4	68.6	51.2	42.4	65.6	45.7	32	248	45.7	57.3	48.8	28.7	49.7	59.2
Dual-ViT-S* [67]	–	–	46.5	68.3	51.2	42.2	65.3	46.1	–	–	46.2	67.4	49.9	30.6	49.9	60.9
CSwin-T [11]	42	279	46.7	68.6	51.3	42.2	65.6	45.4	–	–	–	–	–	–	–	–
InternImage-T [56]	49	270	47.2	69.0	52.1	42.5	66.1	45.8	–	–	–	–	–	–	–	–
SMT-S [37]	40	265	47.8	69.5	52.1	43.0	66.6	46.1	–	–	–	–	–	–	–	–
BiFormer-S [75]	–	–	47.8	69.8	52.3	43.2	66.8	46.5	–	–	45.9	66.9	49.4	30.2	49.6	61.7
RMT-S	46	262	49.0	70.8	53.9	43.9	67.8	47.4	36	244	47.8	69.1	51.8	32.1	51.8	63.5
Swin-S [38]	69	359	45.7	67.9	50.4	41.1	64.9	44.2	60	339	44.5	66.1	47.4	29.8	48.5	59.1
ScalableViT-B [65]	95	349	46.8	68.7	51.5	42.5	65.8	45.9	85	330	45.8	67.3	49.2	29.9	49.5	61.0
InternImage-S [56]	69	340	47.8	69.8	52.8	43.3	67.1	46.7	–	–	–	–	–	–	–	–
CSwin-S [11]	54	342	47.9	70.1	52.6	43.2	67.1	46.2	–	–	–	–	–	–	–	–
Dual-ViT-B* [67]	–	–	48.4	69.9	53.3	43.4	66.7	46.8	–	–	47.4	68.1	51.2	29.6	51.9	63.1
BiFormer-B [75]	–	–	48.6	70.5	53.8	43.7	67.6	47.1	–	–	47.1	68.5	50.4	31.3	50.8	62.6
RMT-B	73	373	51.1	72.5	56.1	45.5	69.7	49.3	63	355	49.1	70.3	53.0	32.9	53.2	64.2
Swin-B [38]	107	496	46.9	69.2	51.6	42.3	66.0	45.5	98	477	45.0	66.4	48.3	28.4	49.1	60.6
PVTv2-B5 [54]	102	557	47.4	68.6	51.9	42.5	65.7	46.0	–	–	–	–	–	–	–	–
Focal-B [63]	110	533	47.8	70.2	52.5	43.2	67.3	46.5	101	514	46.3	68.0	49.8	31.7	50.4	60.8
MPViT-B [32]	95	503	48.2	70.0	52.9	43.5	67.1	46.8	85	482	47.0	68.4	50.8	29.4	51.3	61.5
CSwin-B [11]	97	526	48.7	70.4	53.9	43.9	67.8	47.3	–	–	–	–	–	–	–	–
InternImage-B [56]	115	501	48.8	70.9	54.0	44.0	67.8	47.4	–	–	–	–	–	–	–	–
RMT-L	114	557	51.6	73.1	56.5	45.9	70.3	49.8	104	537	49.4	70.6	53.1	34.2	53.9	65.2

Table 3. Comparison to other backbones using RetinaNet and Mask R-CNN on COCO val2017 object detection and instance segmentation.

Backbone	Params FLOPs		Mask R-CNN 3×+MS					
	(M)	(G)	AP^b	AP_{50}^b	AP_{75}^b	AP^m	AP_{50}^m	AP_{75}^m
Swin-T [38]	48	267	46.0	68.1	50.3	41.6	65.1	44.9
Focal-T [63]	49	291	47.2	69.4	51.9	42.7	66.5	45.9
NAT-T [21]	48	258	47.8	69.0	52.6	42.6	66.0	45.9
GC-ViT-T [22]	48	291	47.9	70.1	52.8	43.2	67.0	46.7
MPViT-S [32]	43	268	48.4	70.5	52.6	43.9	67.6	47.5
SMT-S [37]	40	265	49.0	70.1	53.4	43.4	67.3	46.7
CSwin-T [11]	42	279	49.0	70.7	53.7	43.6	67.9	46.6
InternImage-T [56]	49	270	49.1	70.4	54.1	43.7	67.3	47.3
RMT-S	46	262	50.7	71.9	55.6	44.9	69.1	48.4
ConvNeXt-S [39]	70	348	47.9	70.0	52.7	42.9	66.9	46.2
NAT-S [21]	70	330	48.4	69.8	53.2	43.2	66.9	46.4
Swin-S [38]	69	359	48.5	70.2	53.5	43.3	67.3	46.6
InternImage-B [56]	69	340	49.7	71.1	54.5	44.5	68.5	47.8
SMT-B [37]	52	328	49.8	71.0	54.4	44.0	68.0	47.3
CSwin-S [11]	54	342	50.0	71.3	54.7	44.5	68.4	47.7
RMT-B	73	373	52.2	72.9	57.0	46.1	70.4	49.9

Table 4. Comparison to other backbones using Mask R-CNN with "3×+MS" schedule.

Backbone	Params FLOPs		Cascade Mask R-CNN 3×+MS					
	(M)	(G)	AP^b	AP_{50}^b	AP_{75}^b	AP^m	AP_{50}^m	AP_{75}^m
Swin-T [38]	86	745	50.5	69.3	54.9	43.7	66.6	47.1
NAT-T [21]	85	737	51.4	70.0	55.9	44.5	67.6	47.9
GC-ViT-T [22]	85	770	51.6	70.4	56.1	44.6	67.8	48.3
SMT-S [37]	78	744	51.9	70.5	56.3	44.7	67.8	48.6
Ortho-S [27]	81	755	52.3	71.3	56.8	45.3	68.6	49.2
HorNet-T [45]	80	728	52.4	71.6	56.8	45.6	69.1	49.6
CSwin-T [11]	80	757	52.5	71.5	57.1	45.3	68.8	48.9
RMT-S	83	741	53.2	72.0	57.8	46.1	69.8	49.8
Swin-S [38]	107	838	51.9	70.7	56.3	45.0	68.2	48.8
NAT-S [21]	108	809	51.9	70.4	56.2	44.9	68.2	48.6
GC-ViT-S [22]	108	866	52.4	71.0	57.1	45.4	68.5	49.3
DAT-S [58]	107	857	52.7	71.7	57.2	45.5	69.1	49.3
HorNet-S [45]	108	827	53.3	72.3	57.8	46.3	69.9	50.4
UniFormer-B [33]	107	878	53.8	72.8	58.5	46.4	69.9	50.4
RMT-B	111	852	54.5	72.8	59.0	47.2	70.5	51.4

Table 5. Comparison to other backbones using Cascade Mask R-CNN with "3×+MS" schedule.

Model	Params(M)	FLOPs(G)	Top1-acc(%)	AP^b	AP^m	mIoU(%)
RMT-T	14.3	2.5	82.4	47.1	42.6	46.4
ReSA->Attention	14.3	2.5	81.6	44.6	40.7	43.9
Softmax ->Gate	15.6	2.7	Nan	—	—	—
w/o LCE	14.2	2.4	82.1	46.7	42.3	46.0
w/o CPE	14.3	2.5	82.2	47.0	42.4	46.4
w/o Stem	14.3	2.2	82.2	46.8	42.3	46.2

Table 6. Ablation study

Backbone	Semantic FPN 80k		
	Params(M)	FLOPs(G)	mIoU(%)
ResNet18 [23]	15.5	32.2	32.9
PVTv2-B1 [54]	17.8	34.2	42.5
VAN-B1 [19]	18.1	34.9	42.9
EdgeViT-S [41]	16.9	32.1	45.9
RMT-T	17.0	33.7	46.4
DAT-T [58]	32	198	42.6
CrossFormer-S [55]	34	221	46.0
UniFormer-S [33]	25	247	46.6
CSWin-T [11]	26	202	48.2
Shuted-S [46]	26	183	48.2
RMT-S	30	180	49.4
DAT-S	53	320	46.1
UniFormer-B [33]	54	350	47.7
CrossFormer-B [55]	56	331	47.7
CSWin-S [11]	39	271	49.2
RMT-B	57	294	50.4
DAT-B	92	481	47.0
CrossFormer-L	95	497	48.7
CSWin-B [11]	81	464	49.9
RMT-L	98	482	51.4

Table 7. Comparison with the state-of-the-art on ADE20K. The framework is SemanticFPN.

Results. The results of semantic segmentation can be found in Tab. 7 and Tab. 8. All the FLOPs are measured with the resolution of 512×2048 . All our models achieve the best performance in all comparisons. Specifically, our RMT-S exceeds Shunted-S for **+1.2** mIoU with Semantic FPN. Moreover, our RMT-B outperforms the recent InternImage-S for **+1.3** mIoU. All the above results demonstrate our model’s superiority in dense prediction.

4.4. Ablation Study

ReSA. We verify the impact of Retentive Self-Attention on the model, as shown in the Tab. 6. ReSA improve the model’s performance in image classification and downstream tasks.

Softmax. In RetNet, Softmax is abandoned in favor of a non-linear gating function. We attempt to replace Soft-

Backbone	UpNet 160k		
	Params(M)	FLOPs(G)	mIoU(%)
DAT-T [58]	60	957	45.5
NAT-T [21]	58	934	47.1
InternImage-T [56]	59	944	47.9
MPViT-S [32]	52	943	48.3
HorNet-T [45]	55	924	49.2
SMT-S [37]	50	935	49.2
RMT-S	56	937	49.8
DAT-S [58]	81	1079	48.3
SMT-B [37]	62	1004	49.6
HorNet-S [45]	85	1027	50.0
InterImage-S [56]	80	1017	50.2
MPViT-B [32]	105	1186	50.3
CSWin-S [11]	65	1027	50.4
RMT-B	83	1051	51.5

Table 8. Comparison with the state-of-the-art on ADE20K. The framework is UpNet.

max with this gating function in ReSA, but we find that the model utilizing the gating function is unable to undergo stable training in our architecture.

LCE&CPE&Stem. We have conducted ablation experiments on the LCE, CPE, and Stem components. The experimental results indicate that all three components contribute to the improvement of model performance to a certain extent.

5. Conclusion

We propose RMT, a vision backbone that integrates retentive network and Vision Transformer. RMT introduces explicit decay related to distance, which brings spatial prior knowledge to visual models. The new mechanism is called Retentive Self-Attention (ReSA). To reduce the complexity of the model, RMT also employs a method that decomposes the ReSA into two axes. Extensive experiments validate the effectiveness of RMT, especially in downstream tasks such as object detection, where RMT demonstrates significant advantages. Our work is still in progress.

References

- [1] Moab Arar, Ariel Shamir, and Amit H. Bermano. Learned queries for efficient local attention. In *CVPR*, 2022. [4](#)
- [2] Zhaowei Cai and Nuno Vasconcelos. Cascade r-cnn: Delving into high quality object detection. In *CVPR*, 2018. [5](#)
- [3] Chun-Fu (Richard) Chen, Rameswar Panda, and Quanfu Fan. RegionViT: Regional-to-Local Attention for Vision Transformers. In *ICLR*, 2022. [1, 4](#)
- [4] Kai Chen, Jiaqi Wang, Jiangmiao Pang, et al. MMDetection: Open mmlab detection toolbox and benchmark. *arXiv preprint arXiv:1906.07155*, 2019. [5](#)
- [5] Xiangxiang Chu, Zhi Tian, Yuqing Wang, Bo Zhang, Haibing Ren, Xiaolin Wei, Huaxia Xia, and Chunhua Shen. Twins: Revisiting the design of spatial attention in vision transformers. In *NeurIPS*, 2021. [2](#)
- [6] Xiangxiang Chu, Zhi Tian, Bo Zhang, Xinlong Wang, and Chunhua Shen. Conditional positional encodings for vision transformers. In *ICLR*, 2023. [2, 4](#)
- [7] MMSegmentation Contributors. Mmsegmentation, an open source semantic segmentation toolbox, 2020. [5](#)
- [8] Ekin D Cubuk, Barret Zoph, Jonathon Shlens, et al. RandAugment: Practical automated data augmentation with a reduced search space. In *CVPRW*, 2020. [5](#)
- [9] Jia Deng, Wei Dong, Richard Socher, et al. Imagenet: A large-scale hierarchical image database. In *CVPR*, 2009. [5](#)
- [10] Mingyu Ding, Bin Xiao, Noel Codella, et al. Davit: Dual attention vision transformers. In *ECCV*, 2022. [4](#)
- [11] Xiaoyi Dong, Jianmin Bao, Dongdong Chen, et al. Cswin transformer: A general vision transformer backbone with cross-shaped windows. In *CVPR*, 2022. [2, 4, 6, 7](#)
- [12] Alexey Dosovitskiy, Lucas Beyer, Alexander Kolesnikov, et al. An image is worth 16x16 words: Transformers for image recognition at scale. In *ICLR*, 2021. [1, 2](#)
- [13] Haoqi Fan, Bo Xiong, Karttikeya Mangalam, Yanghao Li, Zhicheng Yan, Jitendra Malik, and Christoph Feichtenhofer. Multiscale vision transformers. In *ICCV*, 2021. [1](#)
- [14] Qihang Fan, Huaibo Huang, Jiyang Guan, and Ran He. Rethinking local perception in lightweight vision transformer, 2023. [2](#)
- [15] Qihang Fan, Huaibo Huang, Xiaoqiang Zhou, and Ran He. Lightweight vision transformer with bidirectional interaction, 2023. [2, 6](#)
- [16] Li Gao, Dong Nie, Bo Li, and Xiaofeng Ren. Doubly-fused vit: Fuse information from vision transformer doubly with local representation. In *ECCV*, 2022. [2](#)
- [17] SG-Former: Self guided Transformer with Evolving Token Reallocation. Sucheng ren, xingyi yang, songhua liu, xinchao wang. In *ICCV*, 2023. [4](#)
- [18] Jianyuan Guo, Kai Han, Han Wu, Chang Xu, Yehui Tang, Chunjing Xu, and Yunhe Wang. Cmt: Convolutional neural networks meet vision transformers. In *CVPR*, 2022. [2, 4, 6](#)
- [19] Meng-Hao Guo, Cheng-Ze Lu, Zheng-Ning Liu, Ming-Ming Cheng, and Shi-Min Hu. Visual attention network. *arXiv preprint arXiv:2202.09741*, 2022. [4, 7](#)
- [20] Kai Han, An Xiao, Enhua Wu, et al. Transformer in transformer. In *NeurIPS*, 2021. [2](#)
- [21] Ali Hassani, Steven Walton, Jiachen Li, Shen Li, and Humphrey Shi. Neighborhood attention transformer. In *CVPR*, 2023. [4, 6, 7](#)
- [22] Ali Hatamizadeh, Hongxu Yin, Greg Heinrich, Jan Kautz, and Pavlo Molchanov. Global context vision transformers. In *ICML*, 2023. [4, 6](#)
- [23] Kaiming He, Xiangyu Zhang, Shaoqing Ren, and Sun Jian. Deep residual learning for image recognition. In *CVPR*, 2016. [7](#)
- [24] Kaiming He, Georgia Gkioxari, Piotr Dollár, and Ross B. Girshick. Mask r-cnn. In *ICCV*, 2017. [5](#)
- [25] Qibin Hou, Cheng-Ze Lu, Ming-Ming Cheng, and Jiashi Feng. Conv2former: A simple transformer-style convnet for visual recognition. *arXiv preprint arXiv:2211.11943*, 2022. [4](#)
- [26] Gao Huang, Yu Sun, and Zhuang Liu. Deep networks with stochastic depth. In *ECCV*, 2016. [5](#)
- [27] Huaibo Huang, Xiaoqiang Zhou, and Ran He. Orthogonal transformer: An efficient vision transformer backbone with token orthogonalization. In *NeurIPS*, 2022. [4, 6](#)
- [28] Huaibo Huang, Xiaoqiang Zhou, Jie Cao, Ran He, and Tieniu Tan. Vision transformer with super token sampling. In *CVPR*, 2023. [1, 2](#)
- [29] Chao Jia, Yinfai Yang, Ye Xia, Yi-Ting Chen, et al. Scaling up visual and vision-language representation learning with noisy text supervision. In *ICML*, 2021. [2](#)
- [30] Zi-Hang Jiang, Qibin Hou, Li Yuan, Daquan Zhou, Yujun Shi, Xiaojie Jin, Anran Wang, and Jiashi Feng. All tokens matter: Token labeling for training better vision transformers. In *NeurIPS*, 2021. [1, 5](#)
- [31] Alexander Kirillov, Ross Girshick, Kaiming He, and Piotr Dollár. Panoptic feature pyramid networks. In *CVPR*, 2019. [5](#)
- [32] Youngwan Lee, Jonghee Kim, Jeffrey Willette, and Sung Ju Hwang. Mpvit: Multi-path vision transformer for dense prediction. In *CVPR*, 2022. [1, 4, 6, 7](#)
- [33] Kunchang Li, Yali Wang, Peng Gao, Guanglu Song, Yu Liu, Hongsheng Li, and Yu Qiao. Uniformer: Unified transformer for efficient spatiotemporal representation learning, 2022. [4, 5, 6, 7](#)
- [34] Yanghao Li, Chao-Yuan Wu, Haoqi Fan, Karttikeya Mangalam, Bo Xiong, Jitendra Malik, and Christoph Feichtenhofer. Mvitv2: Improved multiscale vision transformers for classification and detection. In *CVPR*, 2022. [1, 4](#)
- [35] Tsung-Yi Lin, Priya Goyal, Ross B. Girshick, and Kaiming He andPiotr Dollár. Focal loss for dense object detection. In *ICCV*, 2017. [5](#)
- [36] Tsung-Yi Lin, Michael Maire, Serge Belongie, et al. Microsoft coco: Common objects in context. In *ECCV*, 2014. [5](#)
- [37] Weifeng Lin, Ziheng Wu, Jiayu Chen, Jun Huang, and Lianwen Jin. Scale-aware modulation meet transformer. In *ICCV*, 2023. [1, 4, 6, 7](#)
- [38] Ze Liu, Yutong Lin, Yue Cao, Han Hu, Yixuan Wei, Zheng Zhang, Stephen Lin, and Baining Guo. Swin transformer: Hierarchical vision transformer using shifted windows. In *ICCV*, 2021. [2, 4, 5, 6](#)

- [39] Zhuang Liu, Hanzi Mao, Chao-Yuan Wu, et al. A convnet for the 2020s. In *CVPR*, 2022. 4, 6
- [40] Jiasen Lu, Christopher Clark, Rowan Zellers, Roozbeh Mottaghi, and Aniruddha Kembhavi. Unified-io: A unified model for vision, language, and multi-modal tasks. In *ICLR*, 2023. 2
- [41] Junting Pan, Adrian Bulat, Fuwen Tan, et al. Edgevits: Competing light-weight cnns on mobile devices with vision transformers. In *ECCV*, 2022. 7
- [42] Zizheng Pan, Jianfei Cai, and Bohan Zhuang. Fast vision transformers with hilo attention. In *NeurIPS*, 2022. 2, 4
- [43] Bo Peng, Eric Alcaide, Quentin Anthony, et al. Rwkv: Reinventing rnns for the transformer era, 2023. 1
- [44] Alec Radford, Jong Wook Kim, Chris Hallacy, Aditya Ramesh, et al. Learning transferable visual models from natural language supervision. In *ICML*, 2021. 2
- [45] Yongming Rao, Wenliang Zhao, Yansong Tang, Jie Zhou, Ser-Lam Lim, and Jiwen Lu. Hornet: Efficient high-order spatial interactions with recursive gated convolutions. In *NeurIPS*, 2022. 6, 7
- [46] Sucheng Ren, Daquan Zhou, Shengfeng He, Jiashi Feng, and Xinchao Wang. Shunted self-attention via multi-scale token aggregation. In *CVPR*, 2022. 3, 7
- [47] Chenyang Si, Weihao Yu, Pan Zhou, Yichen Zhou, Xin-chao Wang, and Shuicheng YAN. Inception transformer. In *NeurIPS*, 2022. 4, 5
- [48] Yutao Sun, Li Dong, Shaohan Huang, Shuming Ma, Yuqing Xia, Jilong Xue, Jianyong Wang, and Furu Wei. Retentive network: A successor to Transformer for large language models. *ArXiv*, abs/2307.08621, 2023. 1, 2, 3
- [49] Shitao Tang, Jiahui Zhang, Siyu Zhu, et al. Quadtree attention for vision transformers. In *ICLR*, 2022. 4
- [50] Hugo Touvron, Matthieu Cord, Matthijs Douze, et al. Training data-efficient image transformers & distillation through attention. In *ICML*, 2021. 4, 5
- [51] Zhengzhong Tu, Hossein Talebi, Han Zhang, Feng Yang, Peyman Milanfar, Alan Bovik, and Yinxiao Li. Maxvit: Multi-axis vision transformer. In *ECCV*, 2022. 1, 4, 5
- [52] Ashish Vaswani, Noam Shazeer, Niki Parmar, et al. Attention is all you need. In *NeurIPS*, 2017. 1, 2
- [53] Wenhai Wang, Enze Xie, Xiang Li, Deng-Ping Fan, Kaitao Song, Ding Liang, Tong Lu, Ping Luo, and Ling Shao. Pyramid vision transformer: A versatile backbone for dense prediction without convolutions. In *ICCV*, 2021. 5, 6
- [54] Wenhai Wang, Enze Xie, Xiang Li, Deng-Ping Fan, Kaitao Song, Ding Liang, Tong Lu, Ping Luo, and Ling Shao. Pvttv2: Improved baselines with pyramid vision transformer. *Computational Visual Media*, 8(3):1–10, 2022. 2, 4, 6, 7
- [55] Wenxiao Wang, Lu Yao, Long Chen, Binbin Lin, Deng Cai, Xiaofei He, and Wei Liu. Crossformer: A versatile vision transformer hinging on cross-scale attention. In *ICLR*, 2022. 4, 6, 7
- [56] Wenhai Wang, Jifeng Dai, Zhe Chen, Zhenhang Huang, Zhiqi Li, Xizhou Zhu, Xiaowei Hu, Tong Lu, Lewei Lu, Hongsheng Li, et al. Internimage: Exploring large-scale vision foundation models with deformable convolutions. In *CVPR*, 2023. 4, 6, 7
- [57] Haiping Wu, Bin Xiao, Noel Codella, Mengchen Liu, Xiyang Dai, Lu Yuan, and Lei Zhang. Cvt: Introducing convolutions to vision transformers. *arXiv preprint arXiv:2103.15808*, 2021. 3
- [58] Zhuofan Xia, Xuran Pan, Shiji Song, Li Erran Li, and Gao Huang. Vision transformer with deformable attention. In *CVPR*, 2022. 2, 3, 6, 7
- [59] Tete Xiao, Yingcheng Liu, Bolei Zhou, Yuning Jiang, and Jian Sun. Unified perceptual parsing for scene understanding. In *ECCV*, 2018. 5
- [60] Haiyang Xu, Qinghao Ye, Ming Yan, Yaya Shi, Jiabo Ye, Yuanhong Xu, Chenliang Li, Bin Bi, Qi Qian, Wei Wang, Guohai Xu, Ji Zhang, Songfang Huang, Fei Huang, and Jingen Zhou. Mplug-2: A modularized multi-modal foundation model across text, image and video. In *ICML*, 2023. 2
- [61] Chenglin Yang, Yilin Wang, Jianming Zhang, et al. Lite vision transformer with enhanced self-attention. In *CVPR*, 2022. 3
- [62] Chenglin Yang, Siyuan Qiao, Qihang Yu, et al. Moat: Alternating mobile convolution and attention brings strong vision models. In *ICLR*, 2023. 4
- [63] Jianwei Yang, Chunyuan Li, Pengchuan Zhang, Xiyang Dai, Bin Xiao, Lu Yuan, and Jianfeng Gao. Focal self-attention for local-global interactions in vision transformers. In *NeurIPS*, 2021. 4, 6
- [64] Jianwei Yang, Chunyuan Li, Xiyang Dai, and Jianfeng Gao. Focal modulation networks. In *NeurIPS*, 2022. 4
- [65] Rui Yang, Hailong Ma, Jie Wu, Yansong Tang, Xuefeng Xiao, Min Zheng, and Xiu Li. Scalablevit: Rethinking the context-oriented generalization of vision transformer. In *ECCV*, 2022. 4, 6
- [66] Ting Yao, Yingwei Pan, Yehao Li, Chong-Wah Ngo, and Tao Mei. Wave-vit: Unifying wavelet and transformers for visual representation learning. In *Proceedings of the European conference on computer vision (ECCV)*, 2022. 2, 3, 5
- [67] Ting Yao, Yehao Li, Yingwei Pan, Yu Wang, Xiao-Ping Zhang, and Tao Mei. Dual vision transformer. *TPAMI*, 2023. 5, 6
- [68] Weihao Yu, Pan Zhou, Shuicheng Yan, and Xinchao Wang. Inceptionnext: when inception meets convnext. In *CVPR*, 2023. 4
- [69] Li Yuan, Qibin Hou, Zihang Jiang, Jiashi Feng, and Shuicheng Yan. Volo: Vision outlooker for visual recognition. *TPAMI*, 2022. 5
- [70] Sangdoo Yun, Dongyoon Han, Seong Joon Oh, et al. Cutmix: Regularization strategy to train strong classifiers with localizable features. In *ICCV*, 2019. 5
- [71] Hongyi Zhang, Moustapha Cisse, Yann N Dauphin, et al. Mixup: Beyond empirical risk minimization. In *ICLR*, 2018. 5
- [72] Pengchuan Zhang, Xiyang Dai, Jianwei Yang, Bin Xiao, Lu Yuan, Lei Zhang, and Jianfeng Gao. Multi-scale vision longformer: A new vision transformer for high-resolution image encoding. In *ICCV*, 2021. 3
- [73] Zhun Zhong, Liang Zheng, Guoliang Kang, et al. Random erasing data augmentation. In *AAAI*, 2020. 5

- [74] Bolei Zhou, Hang Zhao, Xavier Puig, et al. Scene parsing through ade20k dataset. In *CVPR*, 2017. [5](#)
- [75] Lei Zhu, Xinjiang Wang, Zhanghan Ke, Wayne Zhang, and Rynson Lau. Biformer: Vision transformer with bi-level routing attention. In *CVPR*, 2023. [1](#), [4](#), [5](#), [6](#)